CHILEAN JOURNAL of AGRICULTURAL RESEARCH

CHILEANJAR
CHILEAN JOURNAL of AGRICULTURAL RESEARCH

RESEARCH ARTICLE

Silicon-induced leaf structural reinforcement modulates growth, foliar disease and yield performance of rice under nutrient-limited conditions

Arlyna Budi Pustika[1], Lesty Ayu Bidhari[1], Mochammad Arif Subechan[1], Agus Suprihatin[1], Pandu Laksono[2], Setyorini Widyayanti[1], Sudarmaji Sudarmaji[1*], Setia Sari Br. Girsang[1], Amelia Sebayang[3], Idum Satia Santi[4], Kristamtini Kristamtini[1], Sugeng Widodo[2], Hasil Sembiring[1], Subiyakto Subiyakto[5], and Nurnina Nonci[1]

[1]National Research and Innovation Agency (BRIN), Research Center for Food Crops, Cibinong Bogor, Indonesia.
[2]National Research and Innovation Agency (BRIN), Research Center for Behavioral and Circular Economics, Jakarta, Indonesia.
[3]National Research and Innovation Agency (BRIN), Research Center for Horticulture, Cibinong, Bogor, Indonesia.
[4]Institut Pertanian Stiper, Faculty of Agriculture, Yogyakarta, Indonesia.
[5]National Research and Innovation Agency (BRIN), Research Center for Estate Crops, Cibinong, Bogor, Indonesia.
*Corresponding author (suda019@brin.go.id).
Received: 29 February 2026; Accepted: 4 June 2026, Available online: 3 August 2026. doi:10.4067/S0718-58392026000500708

ABSTRACT

Nutrient imbalance can compromise rice (*Oryza sativa* L.) cultivation, hindering the potential of rice plants to produce optimum grain yield. In this study, Si was added as a supplementary fertilizer to reinforce leaf anatomical structure, modulating growth performance, foliar disease resistance, and yield under nutrient-limited conditions. Four fertilization treatments were evaluated using a randomized complete block design, including the use of conventional NPK with and without Si addition. Its effect on leaf structural reinforcement and nutrient accumulation was assessed. Growth parameters, foliar disease severity, incidence, the area under the disease progress curve (AUDPC), and yield components were evaluated across all phenological stages. The results showed that Si accumulation in the leaf, stress-induced or fertilized, significantly affected Mg (194.8 mg kg^{-1} DW) and Zn (82.9 mg kg^{-1}) without compromising P and K uptake. Structural reinforcements of the leaf evaluated included increased thickness of the cuticle (18.3 µm) and mesophyll (256.2 µm), higher stomatal density (473.9 stomata mm^{-2}), and higher chlorophyll content (15.4 SPAD index). Si modulated vegetative growth and biomass during grain filling. Furthermore, Si accumulation reduced AUDPC values for bacterial red stripe, leaf blight, and narrow brown spot from 771.1 to 159.1 %-days, 119.9 to 9.9 %-days, and 786.1 to 452.1 %-days, respectively, demonstrating high resistance toward foliar diseases. Grain yield at 14% moisture content was similar among treatments (6.15-6.24 t ha^{-1}). Si fertilization increased physiological efficiency, strengthened leaf structural defenses, and reduced disease-induced yield losses. It may be used to compensate for or substitute nutrient deficiencies, potentially reducing the quantity of conventional fertilizer required in agricultural practices.

Key words: AUDPC, leaf anatomy, nutrient imbalance, nutrient-use efficiency, performance stability.

INTRODUCTION

Rice (*Oryza sativa* L.) is a vital food source for over half of the global population. It is crucial for ensuring food security in major consuming regions like Asia. However, despite advancements in breeding and agronomy, global rice production has stagnated in recent years (FAO, 2026). Nutrient imbalance in the field remains a significant factor affecting productivity. Intensive cultivation and imbalanced fertilization in weathered tropical soils increase nutrient depletion. As a high-yielding plant, rice relies heavily on a steady nutrient supply to produce grain. Nutrients are building blocks of the plant's anatomical structure and directly affect its metabolism. Any deficiency in these elements results in the degradation or deformation of the plant structure, significantly reducing metabolic functions such as photosynthesis. A compromised structure (withered leaves, weakened cells) and reduced photosynthesis lead to a higher prevalence of bacterial and fungal foliar diseases, particularly during reproductive stages (Begum et al., 2024). This condition further diminishes the physiological efficiency and yield stability of the crop (Devkota et al., 2019; Connor et al., 2023). While specific fertilization can mitigate these issues, the use of Si is particularly promising due to its unique functionality.

Silicon application has been reported to be beneficial in the cultivation of various commodities. It helps to mitigate plant physiological problems related to nutrient-limited conditions. Si is known for its significant accumulation capacity. It can be accumulated in aerial tissues, contributing to the mechanical strengthening of leaves and other parts of plants. Improvements in plant anatomical structure, in nutrient-limited conditions, are necessary to maintain the required metabolism. In this regard, structure-enhancing compounds such as Si could be added to help maintain the structural integrity of rice plants. Si application is linked to specific anatomical adaptations, such as thicker cuticles, strengthened epidermal layers, and enhanced stomatal characteristics (Blanchart et al., 2020; Chen et al., 2021). These improvements enhance photosynthetic performance, limit pathogen penetration, and increase tolerance toward abiotic stresses (MeCarty et al., 2025). In regard to the nutrient-limited aspect, Si supplementation could maintain photosynthetic activity, ensuring the production of optimum yield. However, the effect of Si on plants is related to various factors such as genetics (Pustika et al., 2026). Thus, the use of Si should be adjusted to match the planting material's characteristics. Until now, comprehensive information on variety-specific Si fertilization for rice, such as in 'Inpari 32', has remained scarce.

'Inpari 32' is among the popular rice varieties currently cultivated by farmers. It is characterized by its high tolerance to bacterial leaf blight and blast disease. In its cultivation, nutrients play an important role in optimizing plant defense mechanisms (Rajareddy et al., 2024). Nutrient-limited conditions may render the resistance of 'Inpari 32' compromised towards these diseases. Previous studies have shown that the benefit of Si fertilization in plants is related to nutrient availability and utilization in the plants. Si was reported to improve the uptake of essential elements like Mg and Zn (Ding et al., 2025). Si fertilization on rice decreases the severity of bacterial leaf blight, brown spot, and blast (Fetene, 2019). However, most studies concentrate on single disease systems, controlled environments, or yield responses in isolation. A study based on the comprehensive integration of nutrient dynamics, leaf anatomical traits, disease progression, and yield formation under practical field conditions should be done to further confirm the effectiveness of Si application in actual rice cultivation conditions (Gao et al., 2023). The results may unlock the possibility of Si acting not only as a fertilizer optimizer but also reducing the reliance of farmers on chemicals.

This study aimed to evaluate the combined effects of Si fertilization on leaf nutrient composition, anatomical characteristics, growth performance, foliar disease development, and yield formation of 'Inpari 32' rice in field conditions. This study provides field-based evidence regarding the role of Si as a performance-stabilizing and disease-reducing factor in nutrient-limited rice systems by simultaneously evaluating physiological, anatomical, pathological, and agronomic responses at critical growth stages.

MATERIALS AND METHODS

Materials

The rice (*Oryza sativa* L.) 'Inpari 32' planting material was obtained from local suppliers (Usaha Tani, Prambanan Indonesia). The NPK 15:10:12 fertilizer (NPK Ponska, PT; Pupuk Indonesia (Persero) Group, Gresik, Indonesia), N fertilizer (Urea Nitrea, PT; Pupuk Kujang, Cikampek Indonesia), silica foliar fertilizer (Pupuk Silika, BrMP Pasca Panen, Bogor, Indonesia) were purchased from local suppliers. Chemicals for analysis were of analytical grade.

Location and time

The study was carried out in Bantul Regency, Special Region of Yogyakarta, Indonesia (7°53'29" S, 110°21'53" E) during the dry season of 2024. The trial field was at an elevation of approximately 37 m a.s.l. The rainfall was 47.9 mm per year with 5.4 rainy days, duration of sunshine of 70.2 h, wind velocity of 3.2 m s^{-1}, atmospheric pressure of 991.8 Pa, average temperature of 26.3 °C, humidity of 80.8%, and the soil pH levels were between 5.6 and 6.8.

Experimental design

The study was carried out utilizing randomized complete block design (RCBD) with a single factor (fertilization treatment). Fertilization treatments were adjusted to replicate the various conditions in the field such as recommended dosage (A), limited dosage (B), limited dosage with Si addition (C), and farmer practice (D). The dosage of fertilizer used for the treatments were as follow: A: N, P_2O_5, K_2O, 144, 32, 38 kg ha^{-1}, respectively; B: N, P_2O_5, K_2O, 164, 25, 30 kg ha^{-1}, respectively; C: N, P_2O_5, K_2O, 164, 25, 30 kg ha^{-1}, respectively, and Si 4.5 L ha^{-1}; D: N, P_2O_5, K_2O, 167, 35, 42 kg ha^{-1}, respectively (Table 1). Each treatment was done in six replicates, yielding a total of 24 experimental units. Each experimental unit was comprised of 100 m^2 area, corresponding to 16 rows with 132 hills.

Table 1. Experimental design, and dosage of NPK, urea, and Si fertilizer applied during the trial.

	Treatment A (Recommended dosage)		Treatment B (Limited dosage)		Treatment C (Limited dosage + Si)		Treatment D (Common practice)	
Application (days post-planting)	Fertilizer type	Dosage	Fertilizer type	Dosage	Fertilizer type	Dosage	Fertilizer type	Dosage
		kg ha^{-1}		kg ha^{-1}				kg ha^{-1}
5	NPK (15:10:12)	320	NPK (15:10:12)	250	NPK (15:10:12)	250 kg ha^{-1}	NPK (15:10:12)	175
							Urea	125
27	Urea	104	Urea	275	Urea	275 kg ha^{-1}	Urea	125
					Si	900 mL ha^{-1}		
33	-	-	-	-	Si	900 mL ha^{-1}	-	-
38	-	-	-	-	Si	900 mL ha^{-1}	-	-
39	Urea	104	-	-	-	-	NPK (15:10:12)	175
45	-	-	-	-	Si	900 mL ha^{-1}	-	-
52	-	-	-	-	Si	900 mL ha^{-1}	-	-

Planting material, land preparation, seedling transplantation, and maintenance

A growing medium consisting of soil, manure, and rice husks (2:1:1 ratio) was used in nursery. The seed was applied with a density of 25 g rice seed per m^2 seed bed. The seedlings were grown and maintained for 18-21 d until ready for transplantation. The experimental fields were prepared as follows: The areas were initially tilled twice with a disc plough and then flooded with water. The field was then puddled with two passes of a rotavator. An experimental unit of 5 × 20 m was prepared with a separation of 30 cm width of embankments between experimental unit and block. Rice was established by manual transplanting of prepared seedlings (2-3 seedlings per hill). The spacing was set using "legowo" method consisted of alternating narrow (0.25 m) and wide rows (0.40 m) of transplanted rice. The seedlings were planted at 0.15 m between rice hills within each row (Girsang et al., 2023). All plots were irrigated (3-5 cm standing water) to avoid water deficit stress. Recommended practices for crop protection were used to minimize crop loss from pests and diseases. Weeding was performed manually every 7 d. Fertilization was done as specified in Table 1.

Sampling and measurement

Hills samples were collected at tillering, panicle initiation, and grain filling stage. Ten hills per plot were analyzed for growth performance (plant height and tiller) and foliar disease severity. Four hills per plot were analyzed for their aboveground biomass. All biomasses were collected at ground level and oven dried to determine the total dry weight. The incidence of diseases was measured by assessing the percentage of symptoms at total plot area of each treatment. Leaves samples were collected at grain filling stage, while the plants were in optimal condition, for the analyses of leaf area, chlorophyl, and leaf anatomy. Leaves for elemental analysis were collected during harvesting and dried in an oven at 50 °C for 3 d. The materials were then powdered and sieved (100-mesh) prior to analysis.

Characterization of the leaf

Leaf sample (three uppermost fully expanded leaves) was subjected to a SPAD-502 Plus meter (Konica Minolta, Tokyo, Japan) for chlorophyl content analysis. For each leaf, three chlorophyll readings were taken around the midpoint on the side of the midrib and averaged as described by Peng et al. (1993). For leaf anatomical analysis, leaf samples were cleaned with distilled water and immersed in 70% ethanol before being processed into a microscope specimen. Stomata, thickness of leaf cuticle, epidermis, and mesophyll were observed by utilizing a digital microscope (OptiLab IRIS-4; PT. Miconos, Yogyakarta, Indonesia) and measured in µm. Elemental analysis was done utilizing a non-destructive X-ray fluorescence (XRF) spectroscopy. The samples (leaves fine powder, 10 g) were subjected to energy dispersive XRF (EDXRF) (Epsilon 4; Malvern Panalytical, Malvern, UK) unit equipped with a Rh tube for elemental analysis. The procedure included X-ray irradiation, atomic excitation, emission of X-ray fluorescence, detection and measurement, followed by spectroscopic analysis. The results were presented as relative percentage of minerals in the samples.

Foliar disease assessment

The occurrence of diseases of bacterial leaf blight (BLB), bacterial red stripe (BRS), and narrow brown spot (NBS) were evaluated at tillering, panicle initiation, and grain filling stage. Disease scoring was done using a standard evaluation system (SES) to measure disease severity (IRRI, 2013). Percent disease index (PDI) was calculated using the formula reported by Wheeler (1969):

$$\text{PDI} = \text{Sum of all ratings} \times 100/\text{Total number of observations} \times \text{Maximum rating scale}$$

The area under the disease progress curve (AUDPC) was calculated based on the disease severity percentage of each disease score taken four times using the formula reported by Shaner and Finney (1977):

$$\text{AUDPC} = \sum_{i=1}^{n} \left(\frac{X_i + X_{i+1}}{2} (t_{i+1} - t_i) \right)$$

where X_i is disease proportion at i, t_i is plant age at i, n is the total number of observations.

The PDI evaluates the prevalence of the disease, while the AUDPC determines the disease progress from the date of symptom appearance and the difference between treatment in terms of rice plant disease response. The incidence of disease (occurrence) was calculated using the following formulas:

$$\text{Disease incidence (\%)} = n \times 100\%/N$$

where n is the number of symptomatic plants, N is the total count of observed plants.

Characterization of the yield

The harvest was done at physiological maturity of the rice plant. Grain yield was evaluated from the middle section of each plot (128 hills, 6.24 m^2). All panicles in the harvest area were collected and threshed. The grain was then measured for its moisture content (MC) and adjusted to 14% for grain yield calculation. Yield components were evaluated from 32 hills (1.56 m^2) in plots. A 40 g subsample of spikelet was used to count the numbers of filled and unfilled spikelet. The result was then referred to as filled-grain percentage.

Yield conversion from plot to t ha^{-1}:

$$\text{Yield (t ha}^{-1}) = \frac{\text{Grain weight (kg)} \times 10\,000}{\text{Plot (m}^2) \times 1000}$$

Moisture content correction to 14% MC:

$$\text{Yield}_{14\%\text{MC}}(\text{t ha}^{-1}) = \text{Yield}_{\text{field}} \times \frac{100 - \text{MC}_{\text{field}}}{100 - 14}$$

Statistical analysis

The ANOVA followed by Duncan multiple range test (DMRT) at the 95% confidence level and Pearson correlation analysis were done using SPSS Version 25 (IBM, Armonk, New York, USA). Principal component analysis based on the spectra of XRF was done using RStudio Version 4.5.0 (RStudio: Integrated Development Environment for R. Posit Software, PBC, Boston, Massachusetts, USA).

RESULTS AND DISCUSSION

Nutrient absorption and accumulation on the leaf

Si application significantly increased the Si content in leaves (Table 2). It was found that Si accumulation in recommended dosage treatments (A) and farmer practice (D) (nutrient-sufficient, 6.5% and 7.1%, respectively) was lower than those of limited dosage treatment (B) and limited dosage with Si addition (C) with nutrient-limited, 7.9% and 8.4%, respectively. Low Si accumulation in the leaves of those treatments corresponded to the nutrient-sufficient condition of the plants. Rice plants are Si accumulators, in which their depositions are commonly centered on epidermal and vascular tissues. The accumulation of Si in rice plants has been reported to occur through active transport mechanisms (Lsi1 and Lsi2). High Si content in the leaves of treatment B was reasonable due to its nutrient-limited nature. Si foliar application thus further increased the Si content as found in treatment C. Considering that Si accumulation in leaves was both a response of defense mechanisms and an induced effect of fertilization, its occurrence might indicate or trigger changes in nutrient absorption and interaction in rice plants.

Table 2. Mineral composition and chlorophyll content of leaves obtained from different fertilization treatments. A: Recommended dosage; B: limited dosage; C: limited dosage with Si supplementation; D: farmer practice; SPAD index: relative chlorophyll content measured using a SPAD meter (dimensionless). Values with different superscript letters within the same column are significantly different according to Duncan's multiple range test (DMRT, $P \leq 0.05$).

Treatment	Content of Si in leaf	Content of P in leaf	Content of K in leaf	Content of Ca in leaf	Content of Mg in leaf	Content of Zn in leaf	Leaf chlorophyll
	%	%	%	%	mg kg^{-1} DW	mg kg^{-1} DW	SPAD index
A	6.5^{a}	0.28^{a}	4.8^{a}	1.8^{b}	53.3^{a}	80.2^{b}	15.0^{ab}
B	7.9^{bc}	0.28^{a}	4.7^{a}	1.5^{a}	183.4^{b}	71.5^{b}	13.3^{a}
C	8.4^{c}	0.26^{a}	4.6^{a}	1.8^{b}	194.8^{b}	82.9^{b}	15.4^{b}
D	7.1^{ab}	0.29^{a}	5.1^{a}	1.6^{a}	53.3^{a}	54.2^{a}	13.5^{ab}

Si application resulted in varied responses in the plants' ability to absorb and accumulate nutrients (Table 2). Si accumulation significantly affected Mg absorption but did not significantly affect the absorption of P and K. For other nutrients such as Ca and Zn, Si accumulation affected the absorption to various extents. Si application and accumulation in the leaves did not disrupt macronutrient uptake pathways, even in nutrient-limited conditions. This was in line with a previous study by Pandey et al. (2024), who found that Si functioned as a beneficial element rather than a competitive ion in the nutrient acquisition of rice. In this regard, Si accumulation and addition might modulate the macronutrient absorption of nutrient-limited treatments to be similar to that of the nutrient-sufficient ones. Conversely, the concentrations of Mg increased in the high Si-accumulating treatments (B and C), and Zn was high in the Si-fertilized treatment (C).

Mg serves as the central atom in the chlorophyll molecule and is crucial for the activation of Rubisco. On the other hand, Zn acts as a cofactor for various enzymes that play roles in photosynthesis and the regulation of oxidative stress. Increased Mg and Zn with Si fertilization indicate modulated photosynthetic activity during nutrient stress. Furthermore, structural integrity of the root membrane and increased transport activity were also reported to be affected by Si fertilization (Pavlovic et al., 2021; Wang et al., 2025). This nutrient-Si synergy was shown by the significant increase in chlorophyll content in treatment C, suggesting modulated stability of the photosynthetic apparatus. On the other hand, chlorophyll content in the nutrient-limited condition (B) remained the lowest. This might be related to Si's function as a Ca substitute. Si can partially replace Ca in sustaining cell wall rigidity via silica-pectin interactions (He et al., 2015; Guerriero et al., 2016; Frew et al., 2018). In this case, Si accumulation in nutrient-limited treatments might function more towards structural integrity, while the higher Si content in treatment C due to Si fertilization functions both on structural integrity and the modulation of the photosynthetic apparatus.

Principal component analysis on nutrient interactions

Principal component analysis of 23 elements showed an overlapping categorization of elemental attributes among the treatments (Figure 1). The first two principal components accounted for a total data variance of 54.9%: PC1 at 39.4% and PC2 at 15.5% (Figure 1). The PC1 was mainly contributed by Fe, Zn, Si, Ti, Co, Ca, and V, and PC2 by Mn, Mg, Si, and Br. All the treatments' categorizations were in the intersection of four quadrants. Treatment A, as the recommended dosage, showed great coverage of elemental attributes, representing nutrient-sufficiency. On the other hand, the common practice condition (C) showed truncated coverage within treatment A, indicating a lower quantity/contribution of several elements. Surprisingly, the limited nutrient treatment (B) showed a vertical shift towards treatments A and D, indicating higher Mn, Mg, Si, Rb, and Br, but lower Cu, Sc, Cr, and Ni. This confirmed that limitations in nutrient supply directly affected the elemental composition of the plants, which might later compromise metabolism. As suspected, Si fertilization helped to modulate the nutrient composition in rice plants, as shown by larger coverage compared to treatments B and D, overlapping the area of the nutrient-sufficient treatment. This confirmed that Si fertilization was able to modulate nutrient uptake in nutrient-limited conditions.

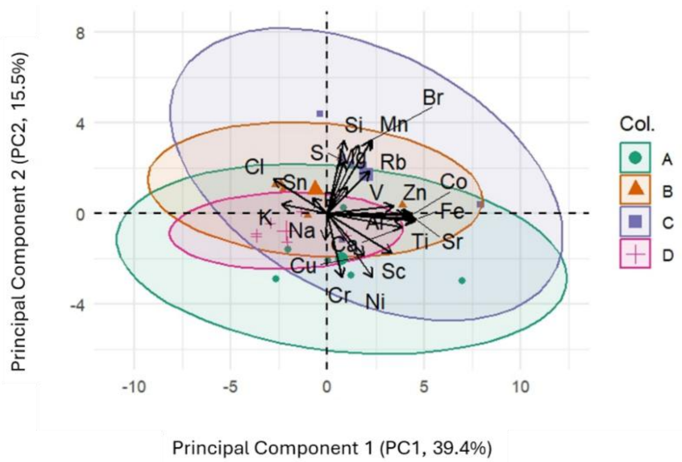

Figure 1. Principal component analysis biplot of X-ray fluorescence (XRF)-derived elemental profiles across various fertilization treatments: Recommended dosage (A), limited dosage (B), limited dosage with Si supplementation (C), farmer practice (D). Ellipses represent 95% confidence intervals for each treatment group.

Radar chart interpretation of the normalized relative elemental composition of the biomass obtained showed that each treatment had different fingerprints (Figure 2). Borges et al. (2020) reported that XRF analysis effectively reveals the presence of macro- and micronutrient elements influencing the physiology of plant tissues and soil. Biomass from treatment D showed high macronutrient spikes (K, Ca, P, S, and Mg) with low micronutrients, indicating that it was obtained from the high-fertilization treatment. This showed that the fertilization dosage of treatment D was "excessive" in terms of macronutrients and thus overtook micronutrient uptake. Treatment A was considered a balanced profile, showing balanced macronutrients and moderate micronutrients. On the other hand, treatment C (Si-fertilized) was characterized by high Fe, Mn, Si, Al, and Mg, indicating high efficiency in nutrient uptake and reinforced structural conformation. This was significantly different from treatment B, which showed enhanced Mg, Si, Mn, and Zn, indicating plant responses to environmental stress. In this context, Fe, Zn, and Mn were previously reported to be important indicators of micronutrient status (Zhang et al., 2025). This finding further confirmed that the occurrence of Fe, Zn, and Mn could differentiate between nutrient-sufficient, nutrient-limited, and nutrient-overloaded conditions. This was in line with the PCA results, which showed that Fe, Zn, and Mn were the determinant factors differentiating the treatments.

	A	B	C	D

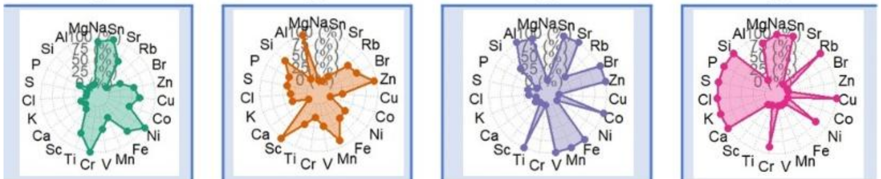

Element	A	B	C	D
Na (%)	0.636	0.359	0.422	0.457
Mg (%)	0.005	0.018	0.019	0.012
Al (%)	0.142	0.129	0.204	0.101
Si (%)	6.470	7.943	8.404	7.074
P (%)	0.281	0.280	0.261	0.285
S (%)	0.124	0.132	0.136	0.134
Cl (%)	1.485	1.658	1.680	2.027
K (%)	4.806	4.697	4.585	5.115
Ca (%)	1.753	1.507	1.777	1.607
Sc (%)	0.001	-	-	-
Ti (%)	0.055	0.042	0.073	0.022
Cr (%)	0.001	-	-	0.001
V (%)	0.001	-	0.002	-
Mn (%)	0.278	0.360	0.460	0.158
Fe (%)	0.676	0.453	0.856	0.237
Ni (%)	0.001	-	-	-
Co (%)	0.002	0.001	0.004	0.001
Cu (%)	0.005	0.004	0.003	0.005
Zn (%)	0.008	0.007	0.008	0.005
Br (%)	0.002	0.003	0.004	0.001
Rb (%)	0.007	0.007	0.007	0.006
Sr (%)	0.006	0.005	0.007	0.003
Sn (%)	-	0.001	-	-
Total (%)	16.745	17.607	18.913	17.252

Figure 2. Radar plot and relative elemental composition of rice leaf samples as determined by X-ray fluorescence (XRF) analysis under four fertilization treatments: Recommended dosage (A), limited dosage (B), limited dosage with Si supplementation (C), farmer practice (D). Each radar axis represents the relative proportion of a given element. Dashes (-) indicate elements below the detection limit of the XRF instrument.

Leaf anatomical structure

Fertilization treatments significantly altered the anatomical structure of the leaves to various extents (Table 3). Leaves obtained from treatment A (recommended dosage of fertilization) were characterized by a thin adaxial cuticle, a moderate abaxial cuticle, increased thickness of the adaxial and abaxial epidermis, a relatively thick parenchyma mesophyll, and a moderate stomatal density. On the contrary, the nutrient-limited treatment (B) produced leaves with relatively low thickness of cuticles (adaxial and abaxial), epidermis (adaxial and abaxial), and parenchyma mesophyll. However, it had a higher stomatal density than that of treatment A. Common fertilization practice (treatment D) produced leaves with significantly thinner parenchyma mesophyll and lower stomatal density than those of other treatments. Interestingly, Si-fertilization helped to increase the thickness of the cuticle, parenchyma mesophyll, and stomatal density, making them higher than other treatments. In nutrient-limited conditions, Si fertilization clearly increased the thickness of adaxial and abaxial cuticles, aligning with the observed silica deposition beneath the cuticular layer (Figure 3). This improvement serves as a physical barrier that minimizes transpirational water loss, restricts excessive ion leakage during nutrient stress, and improves leaf mechanical strength (Souri et al., 2021). The increased thickness of mesophyll parenchyma observed in treatment C (Figure 3) shows that Si enhances internal leaf structural development. Increased thickness of mesophyll layers enhances the volume of chloroplast-rich tissue and improves internal diffusion capacity. This is advantageous during nutrient stress conditions, where photosynthetic efficiency is frequently limited. The simultaneous rise in chlorophyll content indicates that anatomical improvements directly contributed to enhanced photosynthetic capacity, rather than serving solely as structural support.

Table 3. Impact of Si application on the anatomical structure and stomatal density of leaves obtained from different fertilization treatments. A: Recommended dosage; B: limited dosage; C: limited dosage with Si supplementation; D: farmer practice. Light microscopy was used to determine the thickness of the adaxial, abaxial, epidermis, and parenchyma mesophyll in micrometers (μm) from transverse leaf slices. Stomata density was measured in stomata per square millimeter (nr mm^{-2}). Duncan's multiple range test (DMRT, $P \leq 0.05$) indicates substantial differences between values with various superscript letters within the same column.

Treatment	Adaxial cuticle	Abaxial cuticle	Adaxial epidermis	Abaxial epidermis	Parenchyma mesophyll	Stomatal density
	μm	μm	μm	μm	μm	nr mm^2
A	8.0^a	16.2^c	45.1^d	36.6^b	216.5^c	364.6^b
B	13.8^b	11.9^b	19.3^a	25.3^a	197.4^b	395.7^c
C	18.3^d	18.0^d	29.6^b	36.9^b	256.2^d	473.9^d
D	14.9^c	9.5^a	34.6^c	39.9^c	174.4^a	260.4^a

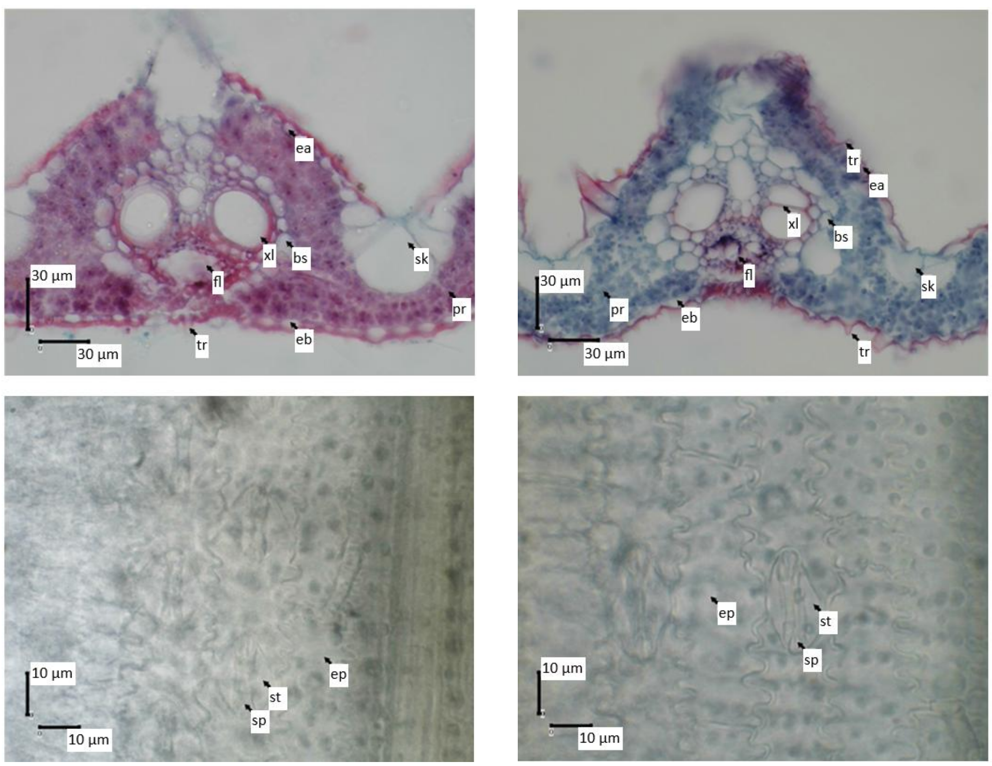

Figure 3. Structure of epidermis, cuticle, and parenchyma mesophyll (top), and density of stoma per mm^2 of leaf obtained from different Si supplementation treatment on nutrient-limited condition (Bottom). ea: Adaxial epidermis; eb: abaxial epidermis; sk: bulliform cell; pr: parenchyma mesophyll; fl: phloem; xl: xylem; tr: trichome; bs: bundle sheath; ep: epidermis; sp: guard cell; st: accessory cell.

The increase in stomatal density in the Si-fertilized treatment was particularly interesting (Table 3, Figure 3). In rice, an increase in stomatal density is directly related to accelerated assimilation capacity, resulting in elevated transpiration rates. These are disadvantages, especially in nutrient-limited conditions. However, Si-induced cuticle thickening, in contrast, reduced excessive water loss. This enabled the rice plants to sustain higher stomatal density without sacrificing water-use efficiency (Chen et al., 2021). This anatomical adjustment indicated that Si-fertilization helped to modulate the balance between gas exchange and transpiration regulation. This is essential during nutrient stress, as impaired nutrient uptake induces stomatal closure and compromises chlorophyll synthesis, further leading to the restriction of photosynthesis (Zhu et al., 2024). In the long term, this would severely affect the production of grain, significantly reducing the yield obtained.

Growth of rice throughout phenological stages

Fertilization treatments influenced the growth of rice plants to different extents, depending on their phenological stages. In terms of plant height, rice that was planted in a nutrient-limited environment (B) had consistently lower plant height ($p < 0.05$) across tillering, panicle initiation (PI), and grain-filling stages than that of the nutrient-sufficient treatments (A and D) (Table 4). On the other hand, treatments A and D produced similar results in terms of plant height. Surprisingly, Si fertilization during the phenological stages of rice growth significantly boosted the plant height despite the plants being treated with nutrient-limited conditions. Treatment C had consistently superior growth performance, exhibiting significantly greater plant height across all growth stages in comparison to other treatments ($p < 0.05$). Increased plant height in Si-fertilized plants was related to enhanced cell elongation and culm rigidity due to silica deposition in cell walls. This improved the mechanical strength of rice plants, sustaining their vertical growth (Tayade et al., 2022).

Table 4. Growth performance of rice across phenological stages on different fertilization treatments. A: Recommended dosage; B: limited dosage; C: limited dosage with Si supplementation; D: farmer practice. Phenological stages: Tillering (55 d after sowing, DAS); panicle initiation (PI, 70 DAS); grain filling (115 DAS). Values with different superscript letters within the same column are significantly different according to Duncan's multiple range test (DMRT, $P \leq 0.05$).

	Plant height (cm)			Number of tillers (nr hill^{-1})			Fresh weight of plant (g)			Dry weight of plant (g)		
Treatment	Tillering	PI	Grain filling	Tillering	PI	Grain filling	Tillering	PI	Grain filling	Tillering	PI	Grain filling
A	42.6^{b}	73.8^{b}	94.2^{b}	17.4^{c}	23.9	30.4^{b}	28.7	125.0	1473.7	5.0	15.6^{bc}	38.3^{a}
B	28.6^{a}	48.4^{a}	80.8^{a}	8.2^{a}	18.9	22.5^{a}	25.3	133.9	1471.0	4.5	13.2^{ab}	36.3^{a}
C	47.5^{c}	81.7^{c}	101.9^{c}	15.7^{bc}	20.9	26.9^{b}	32.5	125.9	1653.7	4.7	16.7^{c}	48.4^{b}
D	46.9^{c}	77.9^{bc}	96.0^{b}	15.0^{b}	20.8	30.3^{b}	37.7	131.6	1614.3	4.3	11.9^{a}	43.8^{ab}

The Si-fertilized treatment showed a result comparable to the number of tillers produced by the nutrient-sufficient treatment ($p > 0.05$). Treatment C exhibited high tiller counts during the tillering and grain-filling stages, similar to those of treatments A and D (Table 4). On the contrary, nutrient-limited conditions consistently produced a lower number of tillers at every phenological stage. The tillering stage in rice is highly dependent on the availability of nutrients, especially N and Mg, due to its direct response to photosynthetic activity. This response aligned with the observed increase in Mg and Zn uptake in treatment C (Table 2). The presence of these nutrients is important as Mg enhances photosynthetic capacity and Zn modulates auxin metabolism and meristem activity. Furthermore, Si fertilization stabilizes root plasma membranes, supporting nutrient uptake in suboptimal conditions (Neu et al., 2017; Dong et al., 2024). In this regard, Si fertilization helped to maintain optimal photosynthetic activity, resulting in the preservation of optimal yield.

Si fertilization significantly increased fresh and dry biomass weight, especially during the grain-filling stage. Treatment C exhibited the highest fresh and dry weights, slightly higher than treatment D. On the other hand, the nutrient-limited treatment showed relatively low fresh and dry biomass weight in all phenological stages, especially in the grain-filling stage. Interestingly, despite the nutrient-limited condition, treatment B showed a fresh weight at the PI and grain-filling stages similar to that of treatment A, which was nutrient-sufficient. However, it was the lowest in terms of dry biomass weight. It should be noted that in treatment B, there was Si accumulation as a result of nutrient stress (Table 2). However, it was not followed by higher efficiency in nutrient uptake (Figure 2). This resulted in the modulation of fresh weight of biomass but a less optimal grain-filling process due to constrained photosynthetic activity. Si-induced thickening of the cuticle and epidermis diminishes non-stomatal water loss, whereas heightened stomatal density improves CO_2 diffusion. This condition enabled rice plants to achieve elevated photosynthetic rates and sustain biomass production despite nutrient stress (Chen et al., 2021). In treatment C, Si fertilization also helped to maintain the uptake of micronutrients, ensuring optimum photosynthetic activity. Furthermore, Si has been reported to improve source-sink balance by postponing leaf senescence and sustaining photosynthetic activity during reproductive phases, thus aiding grain filling in nutrient-limited environments (Chen et al., 2024). This led to the optimum dry weight of the biomass obtained during the grain-filling stage of treatment C (Si fertilized).

Foliar diseases

The analysis of foliar diseases in rice plants subjected to different fertilization treatments revealed significant insights into the correlation between nutrient levels and the severity and incidence of disease. Treatments A and D, characterized by nutrient-sufficient conditions, exhibited consistently higher severity, AUDPC, and incidence of bacterial red stripe, leaf blight, and narrow brown spot disease compared to the nutrient-limited treatments. Nitrogen overload in the soil may be a determining factor influencing this condition. Fetene (2019) reported that excessive N increases the severity and incidence of leaf and panicle blast. Given that treatments A and D utilized high concentrations of NPK and urea, it is plausible that the current dosages were deemed “excessive”, resulting in an increased susceptibility to diseases.

Treatments leading to Si accumulation demonstrated a decreased risk and severity of foliar diseases. Treatments B and C exhibited significantly reduced ($p < 0.05$) severity and incidence of bacterial red stripe, leaf blight, and narrow brown spot across all growth stages compared to treatments A and D (Tables 5 and 6). This was associated with low AUDPC values for all three diseases (Table 7). This aligns with the findings of Panda et al. (2023). Si accumulation not only delayed the onset of disease but also impeded disease progression throughout the cropping cycle. In treatment B, the nutrient-limited conditions utilized may be deemed adequate for disease prevention. Si accumulation resulting from nutrient stress enhances the resistance of rice to diseases.

Table 5. Severity of three major rice foliar diseases at different growth stages of rice on different fertilization treatments. A: Recommended dosage; B: limited dosage; C: limited dosage with Si supplementation; D: farmer practice. Assessment time points: Tillering at 55 d after sowing (DAS), panicle initiation (PI) at 70 DAS, and grain filling at 115 DAS. Disease severity was evaluated as the percentage of leaf area infected (%). Values with distinct superscript letters in the same column indicate significant differences as determined by Duncan’s multiple range test (DMRT, $P \leq 0.05$).

	Bacterial red stripe (%)			Bacterial leaf blight (%)			Narrow brown spot (%)		
Treatment	Tillering	PI	Grain filling	Tillering	PI	Grain filling	Tillering	PI	Grain filling
A	6.5^{b}	14.8^{c}	15.0^{b}	3.7^{a}	20.4^{b}	29.6^{b}	0.0^{a}	4.8^{a}	47.0^{b}
B	3.3^{a}	2.4^{a}	5.0^{a}	1.8^{a}	3.7^{a}	5.6^{a}	0.0^{a}	3.7^{a}	27.2^{a}
C	1.1^{a}	3.7^{ab}	2.4^{a}	0.0^{a}	1.8^{a}	3.7^{a}	0.0^{a}	3.1^{a}	26.3^{a}
D	1.1^{a}	8.9^{b}	25.7^{c}	1.9^{a}	5.6^{a}	7.4^{a}	0.0^{a}	6.9^{a}	48.9^{b}

Table 6. Incidence of three major foliar diseases at different growth stages of rice on different fertilization treatments. A: Recommended dosage; B: limited dosage; C: limited dosage with Si supplementation; D: farmer practice. Assessment time at phenological stages: tillering at 55 d after sowing (DAS), panicle initiation (PI) at 70 DAS, and grain filling at 115 DAS. Disease incidence was determined by calculating the percentage of infected hills relative to the total number of hills evaluated (%). Values with distinct superscript letters in the same column indicate significant differences as determined by Duncan’s multiple range test (DMRT, $P \leq 0.05$).

	Bacterial red stripe (%)			Bacterial leaf blight (%)			Narrow brown spot (%)		
Treatment	Tillering	PI	Grain filling	Tillering	PI	Grain filling	Tillering	PI	Grain filling
A	15.0^{b}	27.5^{b}	40.0^{c}	3.3^{a}	18.3^{b}	26.7^{b}	0.0^{a}	16.7^{a}	40.0^{ab}
B	5.8^{ab}	14.1^{a}	30.5^{bc}	1.7^{a}	3.3^{a}	5.0^{a}	0.0^{a}	13.3^{a}	40.0^{ab}
C	2.5^{a}	10.0^{a}	31.7^{a}	0.0^{a}	1.7^{a}	3.3^{a}	0.0^{a}	8.3^{a}	37.5^{a}
D	3.3^{a}	18.3^{ab}	20.0^{ab}	1.7^{a}	5.0^{a}	6.7^{a}	0.0^{a}	15.0^{a}	46.5^{b}

Table 7. Area under disease progress curve (AUDPC) of three important rice foliar diseases of rice on different fertilization treatments. A: Recommended dosage; B: limited dosage; C: limited dosage with Si supplementation; D: farmer practice. The trapezoidal integration method calculates the area under the disease progress curve (AUDPC) as $\Sigma[(y_i + y_{i+1})/2 \times (t_{i+1} - t_i)]$, where y_i is disease severity (%) at time t_i (d after sowing). Duncan's multiple range test (DMRT, $P \leq 0.05$) indicates substantial differences between values with various superscript letters within the same column.

Treatment	Bacterial red stripe	Bacterial leaf blight	Narrow brown spot
	%-days	%-days	%-days
A	771.1^b	119.90^a	786.1^b
B	219.8^a	22.18^a	478.6^a
C	159.1^a	9.90^a	452.1^a
D	625.2^b	29.60^a	865.7^b

The observed disease response across treatments can be analyzed within a framework of resistance categorization. According to the combined indicators of disease severity, incidence, and AUDPC, which reflect both the magnitude and temporal progression of disease, treatments B and C demonstrated response patterns indicative of a resistant to moderately resistant reaction. This is characterized by low initial severity, minimal disease progression across phenological stages, and suppressed cumulative disease burden. Treatments A and D exhibited response patterns characteristic of a susceptible reaction, demonstrating consistently high severity and incidence from panicle initiation to grain filling, along with significantly elevated AUDPC values. This continuum of resistance and susceptibility across treatments was not due to genetic differences, as all plots utilized the same 'Inpari 32' variety. Instead, it was linked to fertilization-induced changes in host plant physiology and leaf structural integrity. This finding highlights that disease resistance in rice is influenced not only by genotypic factors but also significantly by the nutritional and structural conditions of the plant. Specifically, the extent of Si accumulation and its subsequent effects on cuticle thickness, mesophyll reinforcement, and the availability of metabolic co-factors such as Mg and Zn play crucial roles.

Si fertilization, as implemented in treatment C, significantly decreased the incidence of foliar diseases compared to treatment B. The application of calcium silicate led to a reduction of 30%-60% in neck blast and a 15%-35% decrease in brown spot (Srivani et al., 2024). Si applications similarly decreased the incidence of *Bipolaris oryzae* and grain discoloration by up to 30% (Yan et al., 2018) and improved tolerance to bacterial leaf blight (*Xanthomonas oryzae*). Previous studies have demonstrated the benefits of Si fertilization in relation to various pests and diseases, including false smut (*Ustilaginoidea virens*) and sheath blight (Sarma et al., 2019), as well as straighthead disease through the inhibition of toxic dimethylarsenate accumulation (Gao et al., 2023), leaf folder (Klotzbücher et al., 2018), and stem borer pests (Sarma et al., 2019). In this study, Si fertilization served to enhance the resistance of rice plants to foliar diseases through two complementary mechanisms: A physical barrier effect resulting from Si-induced thickening of the cuticle and mesophyll, which limits pathogen penetration, and a metabolic reinforcement effect facilitated by increased uptake of Mg and Zn, which supports photosynthetic integrity and regulation of oxidative stress. The effect was more pronounced during the panicle initiation and grain filling stages, which are characterized by increased nutrient stress and assimilate competition that typically enhance host susceptibility. Si maintained the structural integrity of leaves, enhanced photosynthetic capacity, and improved nutrient-use efficiency, thereby mitigating disease-induced disruptions in C assimilation and indirectly supporting yield-related processes.

Yield components and grain yield in rice

Yield components and grain yield of the rice obtained from different treatments were mostly similar in almost all aspects ($p > 0.05$), even though some extreme values were also observed (filled grain % and weight of 1000 grains for treatment D, $p < 0.05$). The final grain yield was similar across treatments, varying between 6.15 to 6.24 t ha^{-1} (14% MC). Yield component analysis showed differentiated allocation strategies across treatments. Treatment A yielded the highest number of panicles per hill, while treatment C, despite exhibiting enhanced vegetative growth and biomass accumulation, resulted in a lower number of panicles. Treatment D demonstrated a significantly higher filled-grain percentage and the highest 1000-grain weight, suggesting improved grain filling and distribution towards individual grains. The observed contrasting patterns were in line with the classical source-sink compensation mechanism in rice, where decreases in panicle number are balanced by enhancements in grain filling efficiency or grain size.

The results confirmed that Si acted more as a yield stabilizer/modulator rather than a yield maximizer. Its function in modulating disease resistance and structural enhancement represents a significant agronomic advantage in nutrient-deficient and disease-susceptible conditions. Si enhanced rice productivity by improving physiological efficiency, buffering stress, and increasing yield component plasticity. Insignificant yield variations among treatments indicated the rice's ability to re-adjust sink components in response to enhanced source stability. Si application should be regarded as a strategic input for sustaining yield stability and grain quality in the face of nutrient and biotic stress, rather than merely as a yield-enhancing fertilizer (Liang et al., 2021).

While the harvest index (HI) was not directly measured in this study, the correlation between total aboveground dry biomass at grain filling (Table 4) and final grain yield (Table 8) serves as a valuable proxy for assessing the efficiency of each treatment in converting accumulated biomass into harvestable grain. Treatment C, which yielded the highest dry biomass at grain filling, demonstrated a grain yield statistically comparable to all other treatments ($p > 0.05$). This indicates a relatively lower biomass-to-grain conversion efficiency in relation to its overall vegetative investment. This pattern indicates that a significant portion of the total DM in treatment C was directed towards structural vegetative components. This outcome aligns with the established role of Si in strengthening cell walls, enhancing culm rigidity, and maintaining leaf anatomical integrity, rather than directly enhancing reproductive sink strength. In contrast, treatment D demonstrated the highest filled-grain percentage and 1000-grain weight, despite lower dry biomass accumulation. This suggests a more favorable biomass partitioning toward grain, indicating greater apparent conversion efficiency. Treatment B, despite exhibiting nutrient limitations and the lowest dry biomass accumulation, yielded comparable grain outputs. This indicates that its biomass, although limited in total quantity, was more effectively allocated towards reproductive output, reflecting stress-induced conservative resource allocation strategies in rice. These differential biomass-to-yield relationships across treatments indicate that Si fertilization enhances the physiological quality and structural integrity of source organs, rather than directly increasing sink filling. This reinforces its function as a yield stabilizer rather than a yield maximizer. Future research that includes explicit HI measurements, in conjunction with straw and grain dry weight at final harvest, would significantly enhance the understanding of Si's impact on assimilate partitioning and source-sink dynamics in nutrient-limited environments.

Table 8. Yield components and grain yield of rice on different fertilization treatments. A: Recommended dosage; B: limited dosage; C: limited dosage with Si supplementation; D: farmer practice. Yield was determined from harvested grain per plot and converted to tons per hectare (t ha^{-1}). Yield at 14% moisture content (MC) was calculated as: $Yield_{14}\% = Yield\_field \times (100 - MC\_field)/(100 - 14)$, where MC_field is the grain moisture content (%) measured at harvest using a digital moisture meter. MC: Moisture content. Values with different superscript letters within the same column are significantly different according to Duncan's multiple range test (DMRT, $P \leq 0.05$).

Treatment	Number of panicles per hill	Filled grain	Weight of 1000 grains	Yield	Yield	Yield (14% MC)
	nr $hill^{-1}$	%	g	kg m^{-2}	t ha^{-1}	t ha^{-1}
A	21.5^{b}	88.7^{a}	28.6^{a}	0.74^{a}	7.4^{a}	6.22^{a}
B	20.6^{ab}	82.8^{a}	28.5^{a}	0.71^{a}	7.1^{a}	6.15^{a}
C	18.4^{a}	85.1^{ab}	28.7^{a}	0.71^{a}	7.1^{a}	6.24^{a}
D	19.0^{a}	92.3^{c}	30.4^{b}	0.69^{a}	6.9^{a}	6.23^{a}

Si enhanced photosynthesis and yield production during grain filling stage

The timing of Si application is crucial for optimizing its impact on photosynthetic capacity and yield formation. Among the three phenological stages assessed, the grain-filling stage (115 DAS) was identified as the most responsive period for Si-mediated structural and physiological improvements. Si-fertilized plants (treatment C) demonstrated the highest dry biomass (48.4 g plant^{-1}), plant height (101.9 cm), parenchyma mesophyll thickness (256.2 µm), stomatal density (473.9 nr mm^{-2}), and chlorophyll content (15.4 SPAD index) at this stage, all significantly surpassing the other treatments (p < 0.05). These structural attributes collectively enhance the volume of chloroplast-rich tissue and the capacity for CO_2 diffusion, thereby directly facilitating the photosynthetic rate during the critical phase of rice development that demands the most assimilates. The increased chlorophyll content in treatment C compared to treatment B (13.3 SPAD index) suggests that Si fertilization, rather than solely stress-induced Si accumulation, is essential for maintaining the stability of the photosynthetic apparatus during grain filling. This finding aligns with Chen et al. (2024), who noted that Si fertilization delays leaf senescence and preserves photosynthetic activity during reproductive phases under nutrient-limited conditions.

The pathway to this grain-filling advantage was established earlier. Panicle initiation (70 DAS) signified the beginning of increased disease pressure, as indicated by significantly higher AUDPC values for bacterial red stripe and narrow brown spot in treatments A and D. At this stage, Si fertilization effectively inhibited disease progression, thereby indirectly maintaining functional photosynthetic leaf area, which was subsequently sustained during grain filling. This sequential function of Si, reinforcing structural integrity at panicle initiation and sustaining photosynthetic capacity and biomass accumulation during grain filling, constitutes the primary mechanism by which Si stabilizes yield under nutrient-limited conditions. The elevated Mg uptake in treatment C (194.8 mg kg^{-1} DW), which serves as a cofactor in chlorophyll biosynthesis and Rubisco activation, reinforces photosynthetic maintenance by providing essential enzymatic and pigment-level support during periods of high assimilate demand.

These findings align with an expanding collection of cross-species evidence indicating that Si functions as a broad-spectrum physiological stabilizer. Alharbi et al. (2024) demonstrated that Si application in salt-stressed maize markedly enhanced chlorophyll content and membrane stability index, while concurrently decreasing oxidative damage indicators such as malondialdehyde and hydrogen peroxide. This study underscores the importance of Si in maintaining photosynthetically active tissue under ionic stress. In a complementary context, Celik et al. (2025) demonstrated that Si application enhanced vegetative growth and yield of cauliflower (*Brassica oleracea* var. *botrytis*) under deficit irrigation conditions across various water supply levels, confirming that Si mitigates the negative impacts of resource limitation on crop performance. The Si-mediated cuticle thickening (18.3 µm) and mesophyll reinforcement (256.2 µm) observed in this study are structurally similar to the improvements in water-use efficiency under limited water supply reported by Celik et al. (2025), as both mechanisms minimize non-stomatal water loss while maintaining gas exchange capacity. In all three systems, nutrient-limited rice, salt-stressed maize, and deficit-irrigated cauliflower, Si consistently acted as a physiological stabilizer by enhancing cellular structural integrity, supporting nutrient uptake efficiency, and preserving photosynthetically active tissue during critical growth stages. These convergent findings from both monocots and dicots, as well as various stress types including nutrient, ionic, and water-deficit, indicate that the strategic timing of Si fertilization should align with the reproductive and grain-filling stages to achieve optimal agronomic benefits.

Industrial relevance, cost benefit, and practical recommendations

The function of Si as a metabolic and structural regulator in rice plants under nutrient-limited situations is further supported by this work. Increased micronutrient intake (particularly Mg), thickening of the adaxial cuticle and parenchyma mesophyll, and increased stomatal density were all influenced by Si buildup, whether it resulted from intentional fertilization or stress reactions (Figure 4). Together, these structural changes decreased the frequency and intensity of foliar diseases without appreciably affecting yield and growth performance. As a result, Si fertilization is best suited as an additional input, especially during times of nutrient scarcity, environmental stress, or circumstances that jeopardize the structural integrity of plants. Additionally, its modulatory ability supports the more general goals of precision and environmentally friendly farming methods.

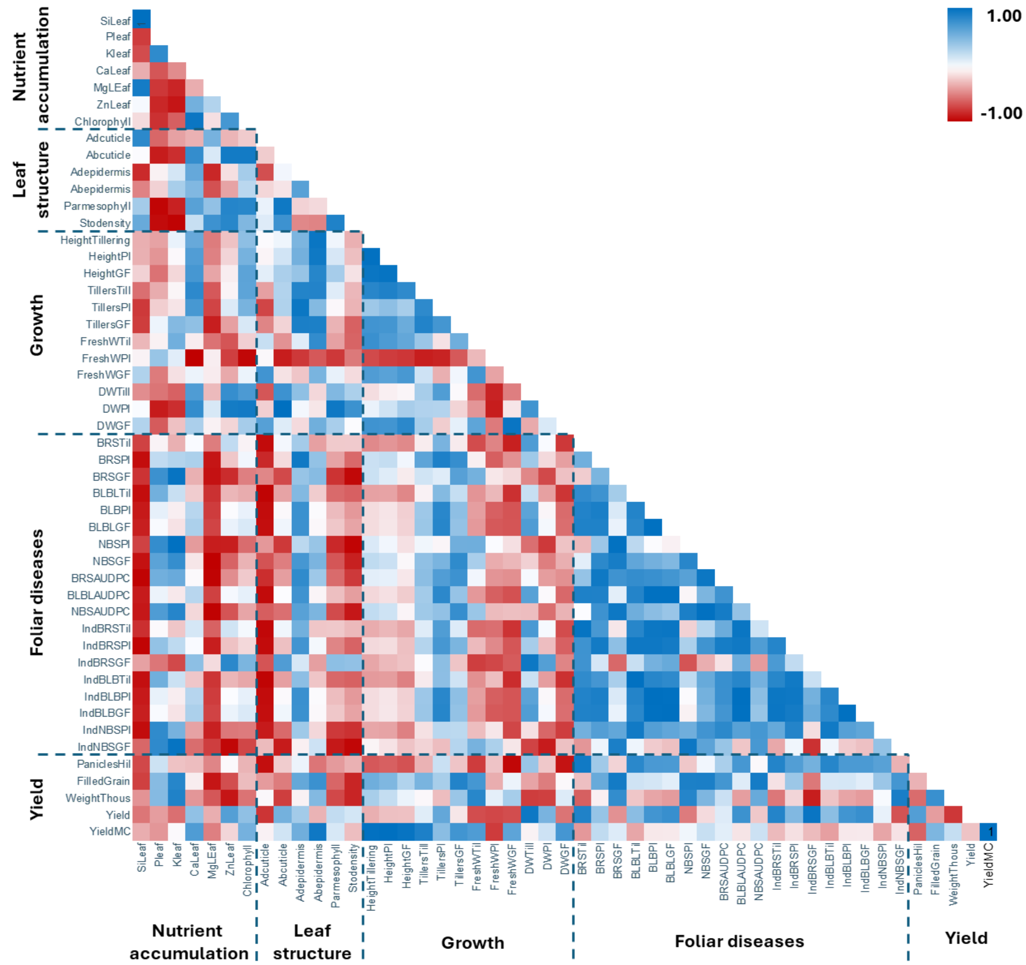

Figure 4. Pearson correlation coefficient heatmap of rice plant nutrient accumulation, leaf anatomical structure, growth, foliar disease, and yield under four fertilization treatments: Recommended dosage (A), limited dosage (B), limited dosage with Si supplementation (C), farmer practice (D). Colour intensity denotes correlation strength and direction, with blue indicating high positive correlation (r = +1.00) and red indicating strong negative correlation (*r* = −1.00). White shows no association. Dashed lines group variables. SiLeaf, PLeaf, KLeaf, CaLeaf, MgLeaf, ZnLeaf: Si, P, K, Ca, Mg, Zn leaf content; Ad: adaxial; Ab: abaxial; Parmesophyll: palisade mesophyll thickness; stodensity: stomatal density; PI: panicle initiation; GF: grain filling; Till: tillering; FreshW: fresh weight; DW: dry weight; BRS: bacterial red stripe; BLB: bacterial leaf blight; NBS: narrow brown spot; AUDPC: area under disease progress curve; Ind: induced; FilledGrain: number of filled grains per panicle; WeightThous: thousand-grain weight; Yield: grain yield; YieldMC: standard moisture content.

Significant differences between theoretical fertilization recommendations and actual field performance were found in the four fertilization situations examined in this study: Recommended dosage, nutrient-limited, nutrient-limited with Si supplementation, and usual farmer practice. Despite providing yields statistically equal to lower-input treatments, treatments A and D, which were intended to simulate nutrient-sufficient circumstances, led to excessive P and K accumulation, paradoxically increasing foliar disease incidence and severity (Figure 4). On the other hand, despite having less vegetative growth than A and D, the nutrient-limited treatment (B) showed surprisingly good foliar disease resistance and yield performance. These results highlight how crucial pre-cultivation soil evaluation is to creating site-specific fertilization strategies that avoid unnecessary overfertilization and enhance soil health. To further define the limits of Si's compensatory modulation capacity, future research using more extreme fertilization gradients is necessary.

From the standpoint of field management, fertilizer application should adhere to site-specific nutrient management principles rather than fixed-rate techniques because fertilizer is the most expensive production input and can degrade soil if applied excessively. The need for conventional nutrients may be somewhat mitigated by Si fertilization: Cuticle thickening brought on by Si accumulation decreases transpirational water loss and, consequently, the plant's dependence on P for osmotic regulation; structurally, Si can replace some functions of N in providing plant rigidity. However, more measurement is needed to determine the exact degree to which Si can make up for lower nutrient inputs.

The agronomic data consistently shows that treatment C (limited NPK + Si supplementation) is the most economical and agronomically balanced choice for smallholder rice farmers, even though a formal economic analysis, which includes cost-benefit ratios, net return per hectare, and break-even Si pricing, falls outside the purview of this study and represents a limitation requiring additional research. Using a lower NPK input (250 kg ha^{-1} NPK + 275 kg ha^{-1} urea) supplemented by Si (4.5 L ha^{-1}), treatment C produced a grain yield of 6.24 t ha^{-1} at 14% moisture content, statistically equivalent to the higher-input treatments A and D ($p > 0.05$). Beyond yield equivalency, treatment C had the lowest disease burden among the three foliar diseases evaluated (BRS AUDPC: 159.1 %-days; BLB AUDPC: 9.9 %-days; NBS AUDPC: 452.1 %-days), suggesting significant pesticide cost savings that bolster its economic argument. Stable biological performance during grain filling, improved biomass accumulation, and enhanced vegetative growth all point to Si compensating for decreased NPK through structural and metabolic modulation rather than just volumetric substitution of fertilizer inputs. Despite requiring the fewest inputs, treatment B continuously showed poorer growth and the lowest chlorophyll content (13.3 SPAD), suggesting a decreased photosynthetic capacity that could impact yield stability under prolonged or increased stress. Therefore, treatment C is the most suitable recommendation for smallholder rice production in nutrient-limited field conditions because it offers the most balanced agronomic profile, including equivalent yield, decreased disease pressure, lower risk of overfertilization, and improved resource-use efficiency.

CONCLUSIONS

This study demonstrates that Si fertilization serves as an effective physiological modulator in 'Inpari 32' rice under nutrient-limited field conditions, enhancing leaf anatomical structure, maintaining nutrient uptake efficiency, inhibiting foliar disease progression, and stabilizing grain yield. Si accumulation in leaves, whether induced by stress or driven by fertilization, serves as a crucial factor. It operates through structural reinforcement of the cuticle and mesophyll, increased stomatal density, and enhanced chlorophyll content, collectively maintaining photosynthetic capacity during critical growth stages. The grain-filling stage is identified as the most responsive period for Si-mediated physiological optimization.

Fertilization with a reduced NPK dosage resulted in the lowest disease burden for all three major foliar diseases assessed, while also yielding grain outputs statistically comparable to those from higher-input treatments. This indicates that Si functions as a yield stabilizer and disease suppressor, rather than a yield maximizer, facilitating agronomically competitive performance with decreased conventional fertilizer input. Excessive NPK application increased disease susceptibility without enhancing yields, highlighting the necessity of soil assessment and site-specific nutrient management before cultivation.

Incorporating Si supplementation into a nutrient-limited fertilization strategy is the most resource-efficient and agronomically balanced method for smallholder rice farmers, providing comparable yields, enhanced disease resistance, and a decreased risk of over-fertilization. Future research should include formal economic analyses and assess Si efficacy across a broader spectrum of fertilization intensities, rice varieties, soil types, and growing seasons to comprehensively determine its scalability as a strategic input in sustainable rice production systems.

Author contribution

Conceptualization: A.B.P. Methodology: A.B.P., A.S., P.L., S.W., S., S.S.B.G., A.Se., I.S.S., K., S.WD., H.S., S.U., N.N. Software: A.B.P., L.A.B., M.A.S., S.W. Validation: A.B.P., L.A.B., M.A.S., A.S., P.L., S.W., S., S.S.B.G., A.Se., K, S.WD., H.S., S.U., N.N. Formal analysis: A.B.P., L.A.B., M.A.S., A.S., P.L., S.W., S., S.S.B.G., A.Se., K., S.WD., H.S., S.U., N.N. Investigation: A.B.P., L.A.B., M.A.S., A.S., P.L., S.W., S., S.S.B.G., A.Se., K., S.WD. Resources: A.B.P., L.A.B., M.A.S., A.S., P.L., S.W., S., S.S.B.G., A.Se., I.S.S., K., S.WD., H.S., S.U., N.N. Data curation: A.B.P., L.A.B., M.A.S., A.S., P.L., S.W., S., S.S.B.G., A.Se., I.S.S., K., S.WD., H.S., S.U., N.N. Writing-

original draft: A.B.P., L.A.B., S.W. Writing-review & editing: A.B.P., L.A.B., M.A.S., A.S., P.L., S.W., S., S.S.B.G., A.Se., I.S.S., K., Su.W., H.S., S.U. N.N. Visualization: A.B.P., L.A.B., M.A.S., S., S.S.B.G., K., Su.W., H.S., S.U., N.N. Supervision: A.B.P., S., S.S.B.G., I.S.S., K., Su.W., H.S., S.U., N.N. Project administration: A.B.P., A.S., P.L., S.S.B.G., A.Se. Funding acquisition: A.B.P., S.S.B.G. All co-authors reviewed the final version and approved the manuscript before submission.

Acknowledgements

This study received support from the funding of Research and Innovation Programs - Third Batch (RIIM-3) of Indonesia National Research and Innovation Agency (BRIN). The author expresses gratitude to Amiliana at Yogyakarta Radiation Laboratory (KSTE Achmad Baiquni) BRIN, Utaminingsih and Prapti at the Faculty of Biology Universitas Gadjah Mada, Yekti Maryani at Universitas Sarjanawiyata Tamansiswa, and Herry Wirianata and Budi at the Faculty of Agriculture Institut Pertanian Stiper Yogyakarta for providing laboratory technical support. Gratitude is extended to Mita Andri Ani and Yosepha Novebriani Jehanim for their technical support at field assessment. We express our gratitude to Dian Palupi and Rosalia Sri Harjanti, the extension officers of Agriculture Services, as well as pak Dalijo and the Manggis Farmer Group for their collaboration in the fieldwork conducted in Bantul.

References

Alharbi, K., Desoky, E-S.M., Rady, M.M., Selem, E., Elrys, A. 2024. Enhancing salt tolerance in maize using co-application of exogenously applied lipoic acid or silicon with soil-based vermicompost tea by reinforcing antioxidant defense mechanisms and regulating plant performance. Chilean Journal of Agricultural Research 84:686-698. doi:10.4067/S0718-58392024000500686.

Begum, M., Li, L., Young, E., Carey, M., Li, G., Zhu, Y-G., et al. 2024. Fertilization enhances grain inorganic arsenic assimilation in rice. Exposure and Health 16:417-430. doi:10.1007/s12403-023-00563-y.

Blanchart, E., Ratsiatosika, O., Raveloson, H., Razafimbelo, T., Razafindrakoto, M., Sester, M., et al. 2020. Nitrogen supply reduces the earthworm-silicon control on rice blast disease in a Ferralsol. Applied Soil Ecology 145:103341. doi:10.1016/j.apsoil.2019.08.003.

Borges, C.S., Weindorf, D.C., Carvalho, G.S., Guilherme, L.R.G., Takayama, T., Curi, N., et al. 2020. Foliar elemental analysis of Brazilian crops via portable X-ray fluorescence spectrometry. Sensors 20(9):2509. doi:10.3390/s20092509.

Celik, Y., Baydar, A., Kayak, N. 2025. Determination of the effects of silicon applications on cauliflower under deficit irrigation conditions. Chilean Journal of Agricultural Research 85:27-33. doi:10.4067/S0718-58392025000100027.

Chen, Y., He, D., Wu, H., Li, Y., Li, P., Huang, H., et al. 2024. Silicon fertiliser application increases the terrestrial ecosystem carbon pool at the global scale. Geoderma 442(2024)116806. doi:10.1016/j.geoderma.2024.116806.

Chen, G., Taherymoosavi, S., Cheong, S., Yin, Y., Akter, R., Marjo, C.E., et al. 2021. Advanced characterization of biomineralization at plaque layer and inside rice roots amended with iron- and silica-enhanced biochar. Scientific Reports 11:159. doi:10.1038/s41598-020-80377-z.

Connor, M., Malabayabas, A.J.B., de Guia, A.H., Wehmeyer, H., Pame, A.R.P., Htwe, N.M., et al. 2023. Environmental, social, and economic challenges in lowland rice production. p. 27-92. In Connor, M., Gummert, M., Singleton, G.R. (eds.) Closing rice yield gaps in Asia, innovations, scaling, and policies for environmentally sustainable lowland rice production. Springer, Cham, Switzerland. doi:10.1007/978-3-031-37947-5.

Devkota, K.P., Pasuquin, E., Elmido-Mabilangan, A., Dikitanan, R., Singleton, G.R., Stuart, A.M., et al. 2019. Economic and environmental indicators of sustainable rice cultivation: A comparison across intensive irrigated rice cropping systems in six Asian countries. Ecological Indicators 105:199-214. doi:10.1016/j.ecolind.2019.05.029.

Ding, Z., Zeng, J., He, Z., Zhu, B., Nie, J., Zhou, Y., et al. 2025. Optimizing fertilization strategies to reduce carbon footprints and enhance net ecosystem economic benefits in ratoon rice systems. Agriculture 15(16):1715. doi:10.3390/agriculture15161715.

Dong, L., Yang, T., Ma, L., Li, R., Feng, Y., Li, Y. 2024. Silicon fertilizer addition can improve rice yield and lodging traits under reduced nitrogen and increased density conditions. Agronomy 14(3):464. doi:10.3390/agronomy14030464.

FAO. 2026. 2026 Global report on food crises. Joint analysis for better decisions. FAO, Rome, Italy. Available at https://openknowledge.fao.org/items/572a3305-91ea-4264-8ef1-b63660ada9d3.

Fetene, D.Y. 2019. Review of the rice blast diseases (*Pyricularia oryzae*) response to nitrogen and silicon fertilizers. International Journal of Research Studies in Agricultural Sciences 5(5):37-44. doi:10.20431/2454-6224.0505005.

Frew, A., Weston, L.A., Reynolds, O.L., Gurr, G.M. 2018. The role of silicon in plant biology: A paradigm shift in research approach. Annals of Botany 121:1265-1273. doi:10.1093/aob/mcy009.

Gao, A., Chen, C., Zhang, H., Yang, B., Yu, Y., Zhang, W., et al. 2023. Multi-site field trials demonstrate the effectiveness of silicon fertilizer on suppressing dimethylarsenate accumulation and mitigating straighthead disease in rice. Environment Pollution 316(120515). doi:10.1016/j.envpol.2022.120515.

Girsang, S.S., Stuart, A.M., Parhusip, D., Manurung, E.D., Miswarti, Pabuayon, I.L.B., et al. 2023. Mid-season adjustment of nitrogen fertilizer for rice with two plant spacings. Field Crops Research 302:109081. doi:10.1016/j.fcr.2023.109081

Guerriero, G., Hausman, J-F., Legay, S. 2016. Silicon and the plant extracellular matrix. Frontiers in Plant Science 7:463. doi:10.3389/fpls.2016.00463.

He, C., Ma, J., Wang, L. 2015. A hemicellulose-bound form of silicon with potential to improve the mechanical properties and regeneration of the cell wall of rice. New Phytologist 206(3):1051-1062. doi:10.1111/nph.13282.

IRRI. 2013. Standard evaluation system for rice. International Rice Research Institute (IRRI), Los Baños, Laguna, Philippines.

Klotzbücher, A., Klotzbücher, T., Jahn, R., Xuan, L.D., Cuong, L.Q., Chien, H.V., et al. 2018. Effects of Si fertilization on Si in soil solution, Si uptake by rice, and resistance of rice to biotic stresses in Southern Vietnam. Paddy and Water Environment 16:243-252. doi:10.1007/s10333-017-0610-2.

Liang, Y., Liao, M., Fang, Z., Guo, J., Xie, X., Xu, C. 2021. How silicon fertilizer improves nitrogen and phosphorus nutrient availability in paddy soil? Journal of Zhejiang University-SCIENCE B (Biomedicine & Biotechnology) 22(7):521-532. doi:10.1631/jzus.B2000708.

MeCarty, J.S., Sharma, N., Kumar, R., Gupta, V., Lalrammawii, C., Farooq, F., et al. 2025. Impact of crop establishment methods, silicon fertilization and silicon solubilizing microbes on growth and economic of basmati rice (*Oryza sativa* L.) Plant Science Today 12(sp4):1-8. doi:10.14719/pst.8645.

Neu, S., Schaller, J., Dudel, E.G. 2017. Silicon availability modifies nutrient use efficiency and content, C:N:P stoichiometry, and productivity of winter wheat (*Triticum aestivum* L.) Scientific Reports 7:40829 doi:10.1038/srep40829.

Panda, S., Kumar, N.R., Pavani, S.L., Ganesan, S., Singh, P.K., Sah, R.P., et al. 2023. Multi-environment evaluation of rice genotypes: Impact of weather and culm biochemical parameters against sheath blight infection. Frontiers in Plant Science 14:1280321. doi:10.3389/fpls.2023.1280321.

Pandey, R., Singh, C., Mishra, S., Abdulraheem, M.I., Vyas, D. 2024. Silicon uptake and transport mechanisms in plants: Processes, applications and challenges in sustainable plant management. Biologia Futura 76:19-31. doi:10.1007/s42977-024-00247-x.

Pavlovic, J., Kostic, L., Bosnic, P., Kirkby, E.A., Nikolic, M. 2021. Interactions of silicon with essential and beneficial elements in plants. Frontiers in Plant Science 12:697592. doi:10.3389/fpls.2021.697592.

Peng, S., Garcia, F.V., Laza, R.C., Cassman, K.G. 1993. Adjustment for specific leaf weight improves chlorophyll meter's estimate of rice leaf nitrogen concentration. Agronomy Journal 85:987-990. doi:10.2134/agronj1993.00021962008500050005x.

Pustika, A.B., Yustyanto, A.F., Sudarmaji, Widyayanti, S., Kristamtini, Nuryanto, B., et al. 2026. Use of Si-based fertilizer significantly improves the performance of 'Sanren' botanical seed-derived shallot. Chilean Journal of Agricultural Research 86:117-128. doi:10.4067/S0718-58392026000100117.

Rajareddy, Gundreddy, Alekhya, G., Kasa, K.R., Dasari, G., Srikanth Reddy, K., et al. 2024. Nutrient strategies for pest resilience in plants: A review. International Journal of Environment and Climate Change 14(5):279-291. doi:10.9734/ijecc/2024/v14i54188.

Sarma, R.S., Shankhdhar, D., Shankhdhar, S.C. 2019. Beneficial effects of silicon fertilizers on disease and insect-pest management in rice genotypes. Journal of Pharmacognosy and Phytochemistry 8(3):358-362.

Shaner, G., Finney, R.E. 1977. The effect of nitrogen fertilization on the expression of slow-mildewing resistance in knox wheat. Phytopathology 67(8):1051-1056.

Souri, Z., Khanna, K., Karimi, N., Ahmad, P. 2021. Silicon and plants: Current knowledge and future prospects. Journal of Plant Growth Regulation 40:906-925. doi:10.1007/s00344-020-10172-7.

Srivani, G., Kumar, G.S., Janaguiraman, M., Arthanari, P.M., Malathi, P., Priya, R.S., et al. 2024. Potency of silicon for enhanced rice productivity: A revelation for global food security. Silicon 16:5501-5523. doi:10.1007/s12633-024-03102-9.

Tayade, R., Ghimire, A., Khan, W., Lay, L., Attipoe, J.Q., Kim, Y. 2022. Silicon as a smart fertilizer for sustainability and crop improvement. Biomolecules 12:1027. doi:10.3390/biom12081027.

Wang, X., Fu, Y., Ruan, Q., Ye, X.H.Q., Yin, Y., Liang, K., et al. 2025. Grain yield and nitrogen use efficiency of a small-grain-weight variety grown under different nitrogen and seeding rates in direct-seeded rice in South China. Food and Energy Security 14:e70139. doi:10.1002/fes3.70139.

Wheeler, B.E.J. 1969. An introduction to plant diseases. John Wiley and Sons, London, UK.

Yan, G-c., Nikolic, M., Ye, M-j., Xiao, Z-x., Liang, Y-c. 2018. Silicon acquisition and accumulation in plant and its significance for agriculture. Journal of Integrative Agriculture 17(10):2138-2150. doi:10.1016/S2095-3119(18)62037-4.

Zhang, C., Charrois, L., Jacquet, J., Sirguey, C., Chen, Z., van der Ent, A. 2025. Monochromatic X-ray fluorescence spectroscopy for major and trace element analysis in plant science applications. Plant and Soil 518:105-120. doi:10.1007/s11104-025-07984-5.

Zhu, P., Chen, S., Shi, Y. 2024. Assessment of nano silicon fertilizer effects on soil nutrients, enzyme activities, and microbial communities. Environmental Science Nano 11:3124-3136. doi:10.1039/d4en00223g.